



OPEN ACCESS

EDITED BY

Matteo Becatti,
University of Firenze, Italy

REVIEWED BY

Federica Riccardo,
University of Turin, Italy
Natalia Rodrigues Mantuano,
University Hospital of Basel, Switzerland

*CORRESPONDENCE

Chiara Falciani,
✉ chiara.falciani@unisi.it

RECEIVED 07 May 2024

ACCEPTED 17 September 2024

PUBLISHED 02 October 2024

CITATION

Rencinai A, Tollapi E, Marianantoni G,
Brunetti J, Henriquez T, Pini A, Bracci L and
Falciani C (2024) Branched oncolytic peptides
target HSPGs, inhibit metastasis, and trigger
the release of molecular determinants of
immunogenic cell death in pancreatic cancer.
Front. Mol. Biosci. 11:1429163.
doi: 10.3389/fmolb.2024.1429163

COPYRIGHT

© 2024 Rencinai, Tollapi, Marianantoni,
Brunetti, Henriquez, Pini, Bracci and Falciani.
This is an open-access article distributed
under the terms of the [Creative Commons
Attribution License \(CC BY\)](https://creativecommons.org/licenses/by/4.0/). The use,
distribution or reproduction in other forums is
permitted, provided the original author(s) and
the copyright owner(s) are credited and that
the original publication in this journal is cited,
in accordance with accepted academic
practice. No use, distribution or reproduction
is permitted which does not comply with
these terms.

Branched oncolytic peptides target HSPGs, inhibit metastasis, and trigger the release of molecular determinants of immunogenic cell death in pancreatic cancer

Alessandro Rencinai, Eva Tollapi, Giulia Marianantoni,
Jlenia Brunetti, Tania Henriquez, Alessandro Pini, Luisa Bracci
and Chiara Falciani*

Department of Medical Biotechnology, University of Siena, Siena, Italy

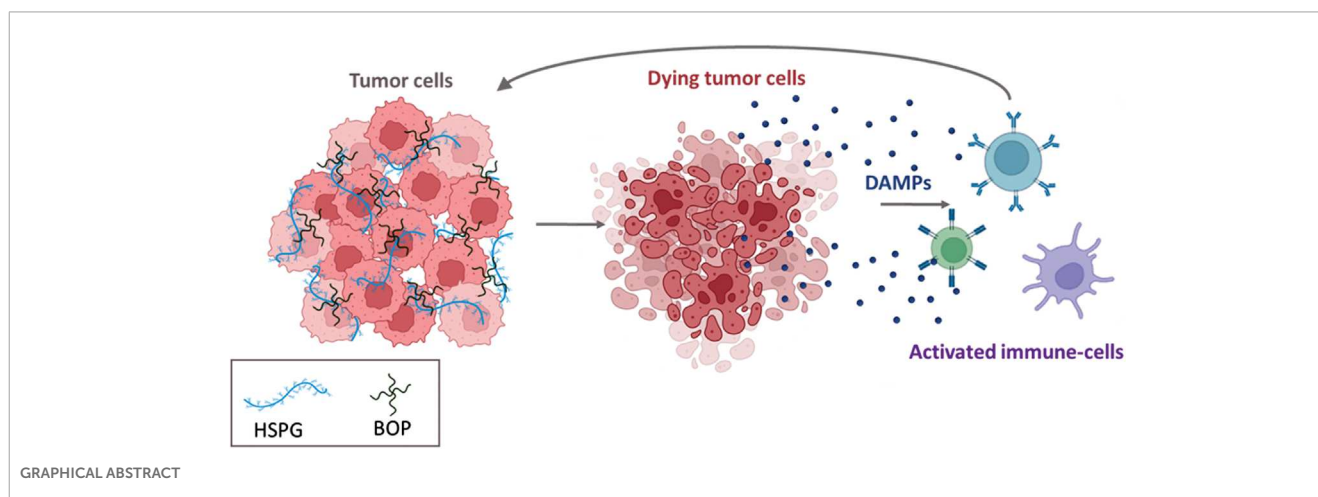
Immunogenic cell death (ICD) can be exploited to treat non-immunoreactive tumors that do not respond to current standard and innovative therapies. Not all chemotherapeutics trigger ICD, among those that do exert this effect, there are anthracyclines, irinotecan, some platinum derivatives and oncolytic peptides. We studied two new branched oncolytic peptides, BOP7 and BOP9 that proved to elicit the release of damage-associated molecular patterns DAMPs, mediators of ICD, in pancreatic cancer cells. The two BOPs selectively bound and killed tumor cells, particularly PANC-1 and Mia PaCa-2, but not cells of non-tumor origin such as RAW 264.7, CHO-K1 and pgsA-745. The cancer selectivity of the two BOPs may be attributed to their repeated cationic sequences, which enable multivalent binding to heparan sulfate glycosaminoglycans (HSPGs), bearing multiple anionic sulfation patterns on cancer cells. This interaction of BOPs with HSPGs not only fosters an anti-metastatic effect *in vitro*, as demonstrated by reduced adhesion and migration of PANC-1 cancer cells, but also shows promising tumor-specific cytotoxicity and low hemolytic activity. Remarkably, the cytotoxicity induced by BOPs triggers the release of DAMPs, particularly HMGB1, IFN- β and ATP, by dying cells, persisting longer than the cytotoxicity of conventional chemotherapeutic agents such as irinotecan and daunorubicin. An *in vivo* assay in nude mice showed an encouraging 20% inhibition of tumor grafting and growth in a pancreatic cancer model by BOP9.

KEYWORDS

immunogenic cell death, pancreatic cancer, oncolytic peptides, danger associated molecular patterns, metastasis

Introduction

The primary explanation for the poor prognosis often associated with pancreatic cancer, particularly pancreatic ductal adenocarcinoma (PDAC), is its immunologically inert nature. PDAC is characterized by a prevalence of immunosuppressive infiltrating cells (Di Federico et al., 2022; Herting et al., 2021;



Yin et al., 2022) and it also has a low mutational burden, resulting in low levels of neoantigens and a compromised capacity for T cell recognition of tumors (Alexandrov et al., 2013; Hou et al., 2022). Consequently, immune checkpoint inhibitors (ICIs), a cornerstone of immunotherapy, have shown little efficacy in PDAC patients (Schizas et al., 2020). Successful stimulation of the tumor immune microenvironment is required for an effective PDAC antitumor immune response (Muller et al., 2022).

Immunogenic cell death (ICD) is a regulated type of cell death that drives antigen-specific immune responses culminating in immunological memory (Kroemer et al., 2022). Various endogenous adjuvant signals, referred to as damage-associated molecular patterns (DAMPs), are released by malignant cells during immunogenic stress or cell death, stimulating the maturation of antigen-presenting cells (Zhou et al., 2019). DAMPs include endoplasmic reticulum proteins, calreticulin (CRT), ATP, high mobility group box 1 (HMGB1), and type I interferon (type I IFN). These DAMPs serve collectively as “eat me” and “find me” signals, attracting antigen-presenting cells to sites of immunogenic cell death induction. This process stimulates the uptake, processing, and cross-presentation of tumor-associated antigens, ultimately eliciting an adaptive immune response (Galluzzi et al., 2017).

ICD-inducing anticancer agents are extremely interesting, especially for “cold cancers,” such as pancreatic cancer, because they exhibit “dual-action”: while directly killing most tumor cells, dying cancer cells act as a sort of vaccine that triggers a specific immune response aimed at eradicating the remaining cancer cells.

Indeed, only some chemotherapeutics can induce intracellular stress pathways that activate a DAMP release in dying cancer cells. Conventional chemotherapeutics that do so include cyclophosphamide, anthracyclines and some platinum derivatives (Galluzzi et al., 2017; Yamazaki et al., 2020). Photodynamic therapy (PDT) (Gomes-da-Silva et al., 2018) and radiotherapy with γ irradiation (Shekarian et al., 2019) have also proved effective in triggering ICD.

The literature contains a vast number of examples of peptides with cytolytic sequences and selectivity for cancer cells (Ghaly et al., 2023; Tornesello et al., 2020; Liu et al., 2023). Most are derived from natural host defence peptides, highly conserved peptides, synthesized by almost all living organisms. They generally consist of

10–30 amino acids that confer a global amphipathic conformation with a positive net charge originating from the high prevalence of cationic (e.g., Lys, Arg) and hydrophobic (e.g., Ala, Val, Gly) amino acids, that allow interaction with biological membranes. These oncolytic peptides can also elicit immunogenic cell death by triggering release of ICD-related DAMPs (Galluzzi et al., 2020; Monroc et al., 2006; Feliu et al., 2010). Many oncolytic peptides are reported to interact with cell surface heparan sulfates of proteoglycans and to penetrate the plasma membrane (Chen et al., 2015; Brunetti et al., 2015; Falciani et al., 2013). These interactions occur between the cationic, basic amino acids on the peptides and the negatively charged sulfates or carboxyl groups of the glycosaminoglycan (GAG) portion of heparan sulfate glycosaminoglycans (HSPGs) and/or sialic acid, typically increased in cancer cells (Galluzzi et al., 2020). HSPGs can therefore function as the initial selective anchoring site for these oncolytic peptides.

One of the limitations of using short linear peptides in clinical settings is their low half-life *in vivo* due to rapid degradation by peptidases and proteases. This restricts their utility to intratumoral administration (Li et al., 2024). Despite the very promising properties of oncolytic peptides being well-established, only one clinical trial has been published (Nielsen et al., 2023) where patients with metastatic soft tissue sarcoma were treated with the combination of an intratumoral injection of oncolytic peptide and adoptive T-cell therapy, in a phase one study (Nielsen et al., 2023).

Tetrameric dendrimeric peptides have much better resistance to hydrolysis than their monomeric counterparts. This feature is due to their steric hindrance that limits interaction with the cleavage site of peptidases (Bracci et al., 2003; Falciani et al., 2007; Paul et al., 2024). Besides, branched peptides enable greater binding avidity because they form polyvalent bonds. The branched structure, with multiple active sequences on the same molecule, also determines higher local concentrations than can't be achieved with linear homologs (Falciani et al., 2007; Paul et al., 2024).

We accordingly synthesized and assessed the cytotoxic specificity of two oncolytic tetrameric peptides against cancer cells. We also investigated their potential antimetastatic effects through interaction with HSPGs, and their ability to induce immunogenic cell death. The efficacy of these peptides was also evaluated in a murine model of pancreatic cancer.

Materials and methods

Peptide synthesis

Linear peptides L7 and L9 and branched oncolytic peptides BOP7 and BOP9 were synthesized on solid-phase by standard Fmoc chemistry on a Syro multiple-peptide synthesizer (MultiSynTech, Witten, Germany). The branched peptides were synthesized on a TentaGel S RAM resin (Rapp Polymere, Tübingen, Germany). For the branched peptides the first two coupling steps were carried out with Fmoc-Lys(Fmoc)-OH to create the branching core. In the synthesis of biotin-conjugate peptides, Fmoc-Lys(Biotin)-OH was used in the initial coupling step, followed by Fmoc-PEG4-OH in the subsequent step, both preceding introduction of the branching core. Sidechain-protecting groups were 2,2,4,6,7-pentamethyldihydrobenzofuran-5-sulfonyl for R, t-butoxycarbonyl for K, Trityl for Q and t-butyl for S. The final product was cleaved from the solid support, deprotected by treatment with TFA containing triisopropylsilane and water (95/2.5/2.5) and precipitated with diethyl ether. Crude peptide was purified by reversed-phase chromatography on a Phenomenex Jupiter C18 column (300 Å, 10 mm, 250, 610 mm), using 0.1% TFA/water as eluent A and methanol as eluent B, in a linear gradient from 80% A to 50% A in 30 min.

Final peptide purity and identity were confirmed by reversed-phase chromatography on a Phenomenex Jupiter C18 analytical column (300 Å, 5 mm), L7 = 16.28 min; L9 = 14.24 min; BOP7 = 20.04 min; BOP9 = 16.44 min, BOP7-Bio = 21.33 min, BOP9-Bio = 19.43 min and by mass spectrometry with a Bruker Daltonics Ultraflex MALDI TOF/TOF: L7 M + (found) = 1274.159; L9 M + (found) = 1289.085; BOP7 M + (found) = 5.425.857; BOP9 M + (found) = 5.486.092; BOP7-Bio M + (found) = 6.028.439; BOP9 M + (found) = 6.088.041.

Stability to serum proteolysis

A pool of sera from healthy volunteers (n = 4) was diluted 25% using RPMI 1640 medium. Each peptide was incubated at 37°C for 4 and 16 h at different concentrations in the diluted serum. Trichloroacetic acid (TCA), diluted 15% in water, was then added to the samples which were then centrifuged at 12,000 × g. The resulting supernatant was diluted 20% with 0.1% TFA in water and used for HPLC analysis. The HPLC spiked peaks were collected and used for MALDI-TOF analysis. Time-zero HPLC and MS-spectroscopy spectra were obtained immediately after mixing each peptide with 25% serum. The presence of the intact peptide was confirmed by MALDI mass spectrometry.

Cell cultures

Cell lines, purchased from The Global Bioresource Center (ATCC, Rockville, MD, United States), were maintained at 37°C in a 5% CO₂ atmosphere.

PANC-1 and Mia PaCa-2 human pancreas adenocarcinoma, RAW 264.7 murine macrophages, CHO-K1, chinese hamster ovary cells and pgsA-745, chinese hamster ovary cell mutant

deficient in xylosyltransferase (UDP-D-xylose: serine-1,3-D-xylosyltransferase), were grown in their recommended medium: Dulbecco's Modified Eagle's Medium (DMEM). Medium was supplemented with 10% fetal bovine serum (FBS), 200 µg/mL glutamine, 100 µg/mL streptomycin and 60 µg/mL penicillin. The culture medium of Mia PaCa-2 was further supplemented with 2.5% horse serum (HS).

PANC-1-*luc2* cells, luciferase-expressing cell line isolated were obtained from PANC-1 cells, transfected with pGL4.51[luc2/CMV/Neo] vector (Promega, Madison, WI, United States) using Lipofectamine™ 3000 Reagent (ThermoFisher), following the manufacturer's instruction.

Flow cytometry

PANC-1, Mia PaCa-2, RAW 264.7 and pgsA-745 cells were seeded 2 × 10⁵ cells/well in 96-well U-bottom plates. They were incubated with different concentrations (10, 2, and 0.4 µM) of biotinylated BOP7 and BOP9 for 30 min at room temperature, followed by incubation with Streptavidin-FITC diluted 1:1,000 (Sigma Aldrich, St. Louis, MO, United States). All dilutions were performed in PBS, containing 5 mM EDTA and 1% BSA. For BOP binding, 7,000 events were evaluated in a Guava easyCyte Flow Cytometer (Millipore). For the competition experiment with heparin, BOP7 and BOP9 were used at 10 µM in the presence of heparin at 5 and 20 µM. Experiments were repeated at least twice and each group evaluation was conducted in duplicate. The results were analysed by FCS Express 6 Flow cytometry software.

BOP binding to heparin - ELISA

BOP7 and BOP9 were diluted in carbonate buffer (pH 9) and used at concentrations of 10, 5, and 1 µg/mL to coat a 96-well ELISA strip plate in which uncoated wells were used as negative controls. The plate was then sealed and incubated overnight at 4°C, then saturated with milk 3% in PBS. The plate was incubated with heparin-biotin sodium salt (Sigma Aldrich) diluted in PBS-BSA 0.3% to 5 µg/mL. After 30 min incubation and washing, streptavidin-POD (Sigma Aldrich) (1:500 in PBS-milk 0.3%) 100 µL/well was added and incubated in the dark for 30 min at 30°C. After washing, 150 µL/well of substrate solution (phosphoric acid buffer, TMB, DMSO, glycerol and H₂O₂) was added and incubated for 5 min. The reaction was quenched with 50 µL/well of HCl 1M and the plate was read at 450 and 650 nm using a microplate spectrophotometer (Multiskan, Thermo Scientific, Waltham, MA, United States). The data was analysed using GraphPad Prism version 9.5.0 software.

Cell viability assays

PANC-1, PANC-1-*luc2*, Mia PaCa-2 or CHO-K1 cells were seeded 5 × 10⁴ cells/well in a standard 96-well plate and incubated overnight at 37°C, 5% CO₂ atmosphere. Each well was treated with 200 µL BOP7 or BOP9 at different concentrations (from 100 to 0.08 µM) and incubated for 24 h. PANC-1 and Mia PaCa-2 were

also tested with linear peptides L7 and L9 at concentrations ranging from 781 to 0.5 μM under the same conditions. Growth inhibition was assessed with a MMT assay (3-(4,5-dimethylthiazol-2-yl)-2,5-diphenyltetrazolium bromide) (Sigma Aldrich). Optical density was measured at 595 and 650 nm with a microplate spectrophotometer (Multiskan, Thermo Scientific). Experiments were repeated twice in quintuplicate. Cell viability was measured by comparing values of treated and untreated cells. IC50 values were calculated by non-linear regression analysis using GraphPad Prism version 9.5.0 software. Untreated cells showed 100% cell viability.

Hemolysis test

Whole human blood was centrifuged at 3,500 rpm for 10 min. After several washings, isolated cells were diluted 1:50 in PBS and added to a flat 96-well plate (100 μL /well). Serial dilutions of the peptides, from 160 μM to the lowest at 0.25 μM , were added. 100% hemolysis was obtained with 1% TritonX 100 in PBS. The plate was incubated at 37°C for 30 min, centrifuged at 2,000 rpm for 5 min and the supernatant analysed using a plate spectrophotometer (Multiskan, Thermo Scientific) at 405 and 490 nm wavelengths.

Adhesion assay

PANC-1 cells were seeded at a concentration of 2×10^6 cell/mL in a flat 96-well plate. Immediately after, 10, 1 and 0.1 μM BOP7 and BOP9 were added to the plate. Untreated cells were used as control. Cells were incubated at 37°C for 4 h and then fixed with 4% PFA-PBS (Sigma Aldrich). The plates were then washed and stained with 100 μL /well 0.1% Crystal Violet (Sigma Aldrich). After treatment with 10% acetic acid the signal was read at 595 nm (Multiskan, Thermo Scientific).

2D migration assay

Two-well silicone inserts (Ibidi GmbH Gräfelfing Germany) were used for this assay. 3×10^4 PANC-1 cells/well were plated in a final volume of 70 μL of culture media for each side of the insert. After 24 h incubation at 37°C, the inserts were removed and BOP7 and BOP9, at the concentration of 1 and 10 μM , were added. The closure of the gap was monitored with a DFC 7000 T microscope (Leica) taking pictures every 30 min for 16 h. The remaining gap was measured with ImageJ.

3D migration assay

The 24-well transwell inserts (Sarstedt Nümbrecht, Germany) were handled according to the manufacturer's instructions. The inserts were coated with Collagen type I (167 $\mu\text{g}/\text{mL}$) (Corning, NY, United States) overnight at 37°C. PANC-1 cells were seeded in the upper chamber at a concentration of 5×10^5 cells/mL together with BOP7 and BOP9 at 0.1, 1, and 10 μM dissolved in DMEM. 600 μL complete media was placed in the lower chamber, and cells were incubated for 24 h at 37°C. Cells on the upper chamber membrane

were then swabbed and the insert was fixed with 4% PFA-PBS and stained with 0.1% Crystal Violet (Sigma Aldrich). Images were taken in bright field mode with a Leica TCS SP5 microscope. The graph was obtained by measuring the color of each well with ImageJ and normalizing all readouts to the untreated wells.

HMGB1 release

PANC-1 cells were seeded 5×10^4 cells/well in a standard 96-well plate and incubated overnight at 37°C in a 5% CO_2 atmosphere. Then they were treated with BOP7, BOP9, daunorubicin hydrochloride (Sigma Aldrich) and irinotecan hydrochloride (Sigma Aldrich) at different concentrations (from 300 to 2 μM in 200 μL) and left for 24 h at 37°C. The following day, release of HMGB1 in the culture medium was assessed with an HMGB1 ELISA kit (IBL International, Hamburg, Germany) in the PANC-1 supernatants, according to the manufacturer's instructions. Optical density was measured at 450 nm with a microplate spectrophotometer (Multiskan, Thermo Scientific). Data was analysed using GraphPad Prism version 9.5.0 software.

IFN- β release ELISA

PANC-1 cells were seeded 5×10^4 cells/well in a 96-well plate and incubated overnight at 37°C in a 5% CO_2 atmosphere. Cells were then treated with BOP7, BOP9, daunorubicin hydrochloride (Sigma Aldrich) and irinotecan hydrochloride (Sigma Aldrich) at different concentrations (from 300 to 2 μM) and left for 24 h at 37°C.

At the same time, a DuoSet ELISA plate (R&D Systems Inc., Minneapolis, MN, United States) for the detection of IFN- β was prepared following the manufacturer's instructions. The plate was sensitized with 100 μL /well of capture antibody for 24 h. PANC-1 supernatants were collected and centrifuged for 5 min at 1,200 rpm, added to the DuoSet plate at 100 μL /well and incubated for 2 h at room temperature. The detection antibody conjugated with streptavidin-peroxidase was then added. After adding the substrate solution, the plate was read at 450 nm using a microplate spectrophotometer (Multiskan, Thermo Scientific). Data was analysed using GraphPad Prism version 9.5.0 software.

Extracellular ATP bioluminescence assay

PANC-1 cells were seeded (10×10^3 cells/well) in an opaque-walled 96-well plate and incubated overnight at 37°C in a 5% CO_2 atmosphere. The following day, each well was treated with 150 μL BOP7, BOP9, daunorubicin hydrochloride (Sigma Aldrich) or irinotecan hydrochloride (cod. PHR2717, Sigma Aldrich) at different concentrations (from 50 to 2 μM). At the same time, each well was incubated with 50 μL RealTime-Glo Extracellular ATP Reagent Substrate (Promega). The plate was incubated at 37° and bioluminescence was measured at 560 nm at different time intervals with a VICTOR NIVO 5S luminometer (Perkin Elmer, Waltham, MA, United States). Data was analysed using GraphPad Prism version 9.5.0 software.

Mouse model of metastases

Female BALB-c nu/nu 5–6 weeks old mice were obtained from Charles River Laboratories Italia s.r.l. All mice were housed in cages in a pathogen-free animal facility according to local and European Ethical Committee guidelines. Tumor cells PANC1-*luc2* were harvested, washed and injected into the caudal vein (iv) ($0.5\text{--}1 \times 10^6$ PANC1-*luc2* cells per mouse/100 μL PBS) and the animals were randomized into two groups of five: 1) Untreated; 2) Treated with BOP9, intraperitoneal 20 mg/kg in 150 μL saline solution.

Treatments were administered every day for the first 5 days, starting 4 h after the transplant, followed by 2 days of rest, and then three treatments again for a total of 18 treatments over 32 days.

Tumor growth was measured using an IVIS Spectrum Imaging System (IVIS, PerkinElmer). Mice were anaesthetized by vaporized isoflurane and injected subcutaneously (s.c.) with D-luciferin (2.5 mg/mouse Promega) in 100 μL PBS vehicle. Images were taken 15 min after Lucifer injection and photon emissions were collected. Bioluminescence was calculated in regions of interest (ROIs) and intensity was recorded for each tumor. Images of the mice were taken every 2–4 days. Treatment and imaging schedule are reported in Figure 5A. The mice were monitored for 32 days then euthanized. Authorization by the Local EC n. 062018.

Statistical analysis

The results were analysed by Student's t-test using GraphPad Prism (GraphPad, San Diego, CA, United States). When comparing more than two groups, one-way analysis of variance (ANOVA) followed by the Dunnett multiple comparisons test was used to detect significant differences between treatment group means. The data is reported with standard deviation (SD).

Results

Synthesis of branched peptides

The peptides were synthesized as tetrabrached structures having four oligomers linked to a branching three-lysine core (Figure 1). The sequences were chosen from a comprehensive open-access database containing information on amino acid sequences, chemical modifications, 3D structures, bioactivities and toxicities of peptides (DBAASP v3.0). The peptides of the database derive from host defense peptides or non-natural libraries of peptides. We selected two sequences LLKKKFKKLQ (L7) and KKKLKFKKLQ (L-9) because they had already demonstrated activity against breast carcinoma, cervical hepatocellular and pancreatic cancer (Feliu et al., 2010). Both sequences were synthesized in linear (L-7 and L-9) and branched form (BOP7 and BOP9) (Figure 1).

Stability of BOPs to blood proteases

Serum was taken as a model of a complex mixture of different proteases to test the stability of BOPs to hydrolysis and compare it with the linear analogues L7 and L9. Tetrabrached

peptides were incubated in serum for 4 and 16 h at 37°C. HPLC analysis followed by mass spectrometry identified a peak indicating intact peptide (Figure 2) up to 16 h. BOP7 and BOP9 were still detectable after 16 h of incubation in serum, differently from the linear analogues that were hydrolyzed before the 16 h. The very short half-life of the linear analogues prevents their further development.

Specific binding of BOPs to cancer cell lines through HSPGs

PANC-1 and Mia PaCa-2 pancreatic cell lines were chosen to test the ability of BOPs to bind human cancer cell lines. FACS analysis confirmed that BOPs bind both cell lines in a dose-dependent manner (Figures 3A, B, E), with stronger binding at 2 and 10 μM for both BOP7 and BOP9.

To assess binding specificity, immortalized mammalian cell lines of non-cancer origin were analysed under the same flow-cytometry conditions. RAW 264.7 macrophage cells showed low BOP7 and BOP9 binding, exhibiting fluorescence intensities more shifted to the isotypic control, compared to PANC-1 and Mia PaCa-2 (Figures 3C, E).

Since cationic peptides preferentially bind negatively-charged targets, among which the sulfated GAG chains of HSPGs could be preferential, we chose the pgsA-745 cell line to control selectivity. These cells are mutants of chinese hamster ovary cells deficient in xylosyltransferase, the enzyme responsible for the first sugar coupling in the synthesis of the polysaccharide chains of HSPGs, therefore they completely lack the GAG chains (Esko et al., 1988; Yang and Wang, 2023). Interestingly, BOP7 and BOP9 showed poor binding activity on pgsA-745 (Figures 3D, E), suggesting that they may target the heparan sulfate chains of HSPGs.

Given the cationic nature of BOPs and their poor binding to pgsA-745, an ELISA assay was conducted to assess their capacity to bind heparin, a commonly used model for studying HSPGs due to their similar chemical structure.

The results demonstrated that both BOPs showed statistically significant binding to heparin across the range of concentrations tested (1.8, 0.90, and 0.2 μM), compared to the control groups, which included uncoated wells and wells lacking heparin. The binding capacity of BOP7 and BOP9 to heparin reached a maximum and plateaued at 0.90 μM (5 $\mu\text{g}/\text{mL}$) (Figure 3F).

To evaluate the ability of BOP7 and BOP9 to bind to HSPGs on the plasma membrane of PANC-1 and Mia PaCa-2 cells, flow cytometry analysis (FACS) was performed employing heparin as an antagonist at two concentrations (5 and 20 $\mu\text{g}/\text{mL}$) during the cell binding assay. At the higher concentration (20 $\mu\text{g}/\text{mL}$), heparin completely antagonized the binding of BOPs to PANC-1 and Mia PaCa-2 cells (Figures 3G, H), reinforcing the hypothesis that BOPs bind HSPGs on the membranes of cancer cells.

Cytotoxicity of BOPs for pancreatic cancer cells

The specific cytotoxicity of BOPs against cancer cells was tested in PANC-1 and Mia PaCa-2 cell lines and IC50 were measured in

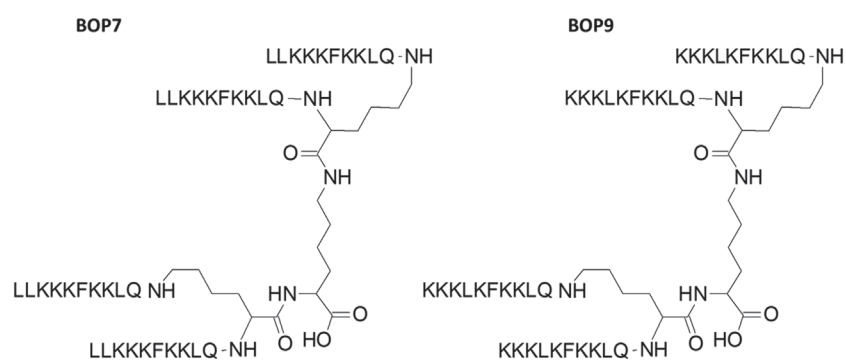
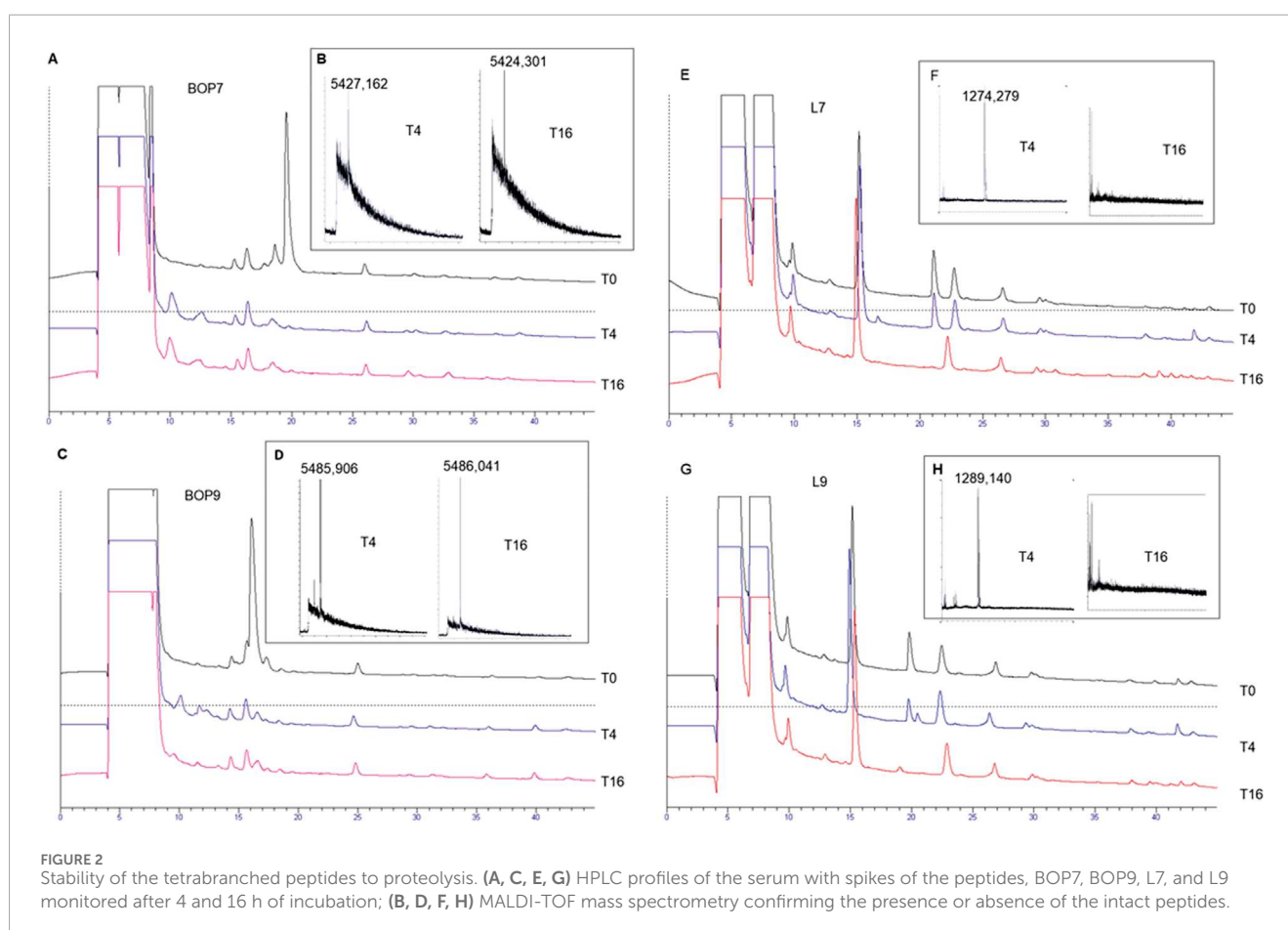


FIGURE 1
Structure of branched oncolytic peptides (BOPs). The three-lysine core allows assembly of four identical copies of the same sequence.



a 24 h treatment experiment. The two BOPs showed micromolar IC₅₀ values. Specifically, BOP7 and BOP9 showed an IC₅₀ of 1.67×10^{-6} M and 8.3×10^{-6} M against PANC-1, respectively; and against Mia PaCa-2 the IC₅₀ was 2.73×10^{-5} M for BOP7 and 1.78×10^{-5} M for BOP9 (Figures 4A, B). Interestingly, the two linear analogues showed no cytotoxic activity against PANC-1 and Mia PaCa-2 (Figures 4C, D, respectively) in 24 h, confirming that the branched design increases biological activity.

CHO-K1 cells were chosen as a model of cells of non-cancer origin to test the safety of BOPs. BOP7 showed an IC₅₀ of 5.0×10^{-3} M and BOP9 of 1.6×10^{-2} M, notably less toxic than against pancreatic cell lines (Supplementary Material 1).

Since many cationic peptides have shown some toxicity towards erythrocytes, BOPs were tested for hemolysis.

The two peptides showed absence of hemolytic activity even at 3 times the highest cytotoxic concentration (Figures 4E, F).

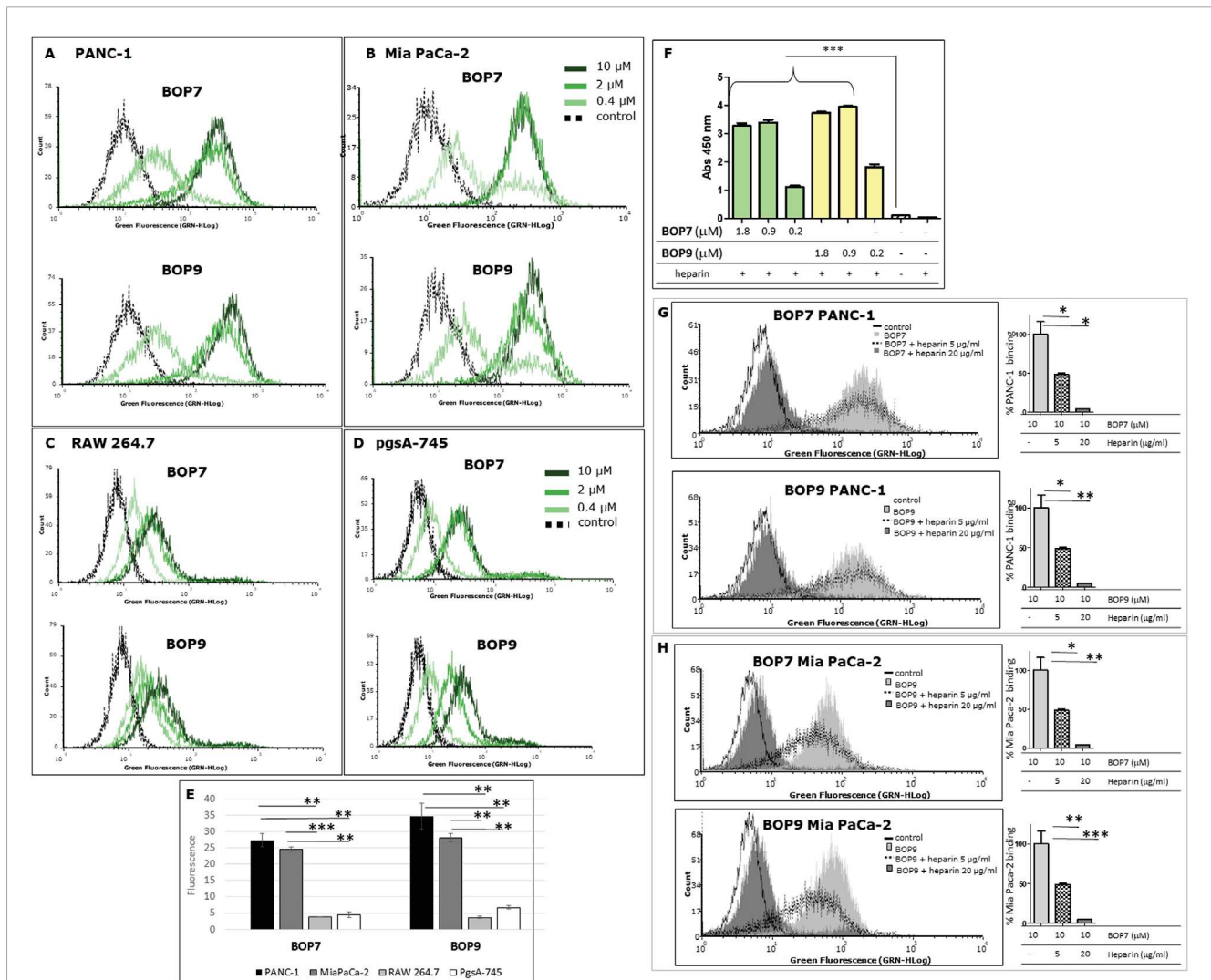
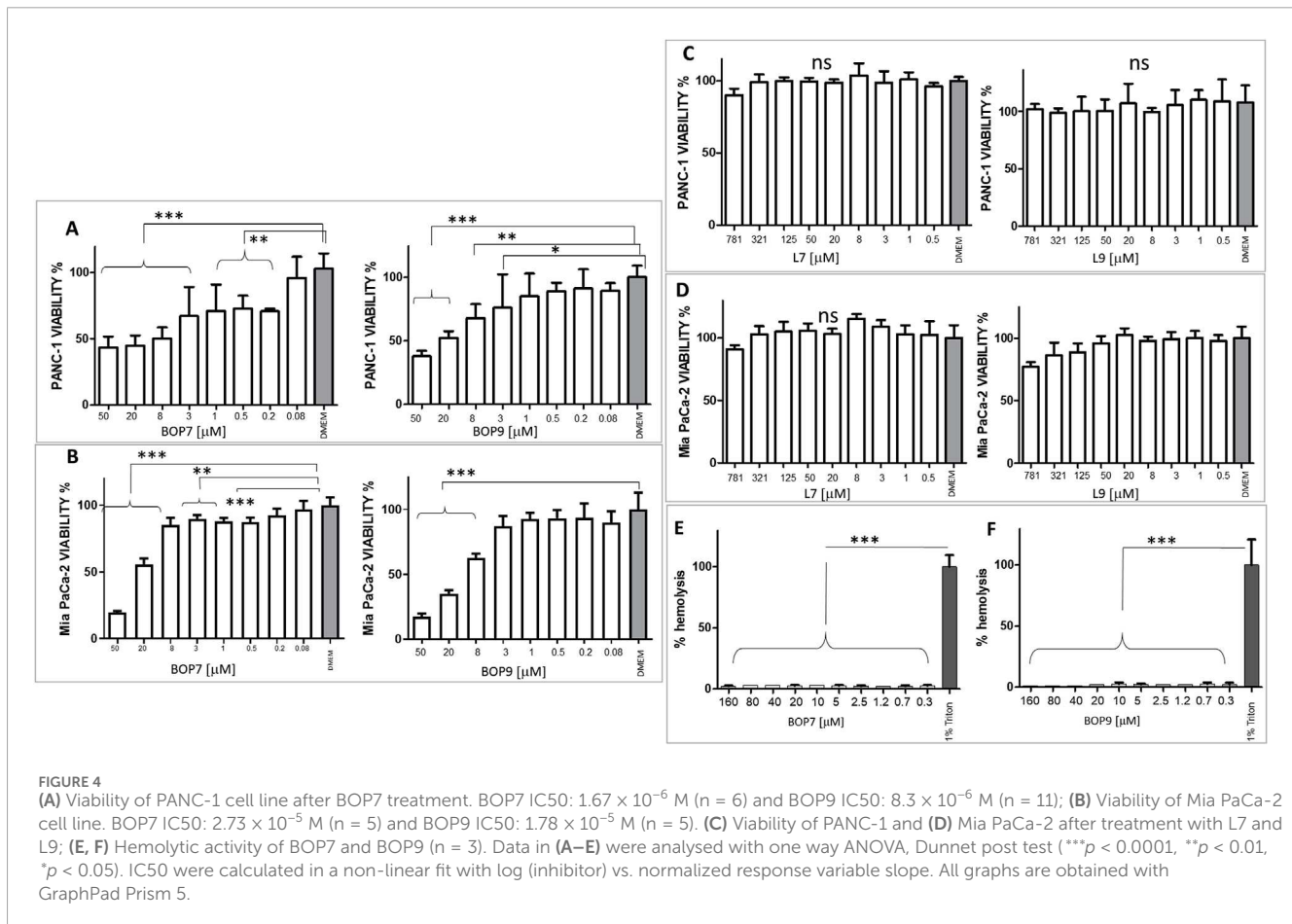


FIGURE 3 (A, B) Flow cytometry analysis of: pancreatic cancer cells, PANC-1 and Mia PaCa-2; (C, D) cells of non-cancer origin, RAW 264.7, murine macrophages and pgsA-745 chinese hamster ovary cell mutant deficient in xylosyltransferase. (E) Quantification of fluorescence intensity of cells treated with 10 μM BOPs, each repeated value (n = 2) was averaged and divided by the value of the untreated cells; (F) ELISA of binding of BOPs to biotinylated heparin; *** $p < 0.0001$ (n = 6), one-way ANOVA and Dunnet post-test. (G, H) Flow cytometry analysis of BOP7 and BOP9 binding to PANC-1 and Mia PaCa-2 cells in the presence of 20 or 5 μg/ml heparin. On the right side of each graph, the quantification of fluorescence intensity, as % of BOPs binding (n = 2).

Effects of BOPs on PANC-1 adhesion and migration

HSPGs play a crucial role in regulating adhesion and migration processes related to invasiveness of cancer cells (Esko et al., 1988; Yang and Wang, 2023). Through their interaction with HSPGs, BOPs may disrupt adhesion and migration mechanisms in cells. Accordingly, we analysed the effect of the peptides on PANC-1 adhesion to the well. BOP7 and BOP9 at 10 μM inhibited adhesion of PANC-1 when incubated at 37°C for 4 h. BOP7 also produced significant inhibition at 1 μM (Figure 5A). Interference with cell migration was studied in a gap-closure model. Migration of PANC-1 cells was significantly inhibited by BOP7 and BOP9 at 10 μM, especially evident in the case of BOP7 (Figure 5B).

To assess whether the effect observed in the two-dimensional migration experiments was correlated with invasiveness *in vitro*, we conducted migration assays using transwell invasion chambers (Figures 5C, D). FBS was used to attract cells and induce their migration from the upper to the lower chamber, passing through the pores of a membrane. In this setting, cells are forced to move, degrade a matrix, collagen type I in this case, and must change shape to squeeze through the pores of the artificial membrane. PANC-1 were seeded on the collagen layer in the upper chamber, and their ability to cross the membrane and reach the lower chamber was measured. BOP7 inhibited PANC-1 3D-migration at a concentration of 10 μM; BOP9 activity was not significant in this setting.



Immunogenic cell death experiments

To evaluate the ability of BOPs to trigger release of DAMPs, PANC-1 cells were treated with different concentrations of BOPs. The effect was compared to that of two chemotherapeutics used in clinical practice: daunorubicin and irinotecan, both widely considered to be powerful inducers of immunogenic cell death.

HMGB1 release

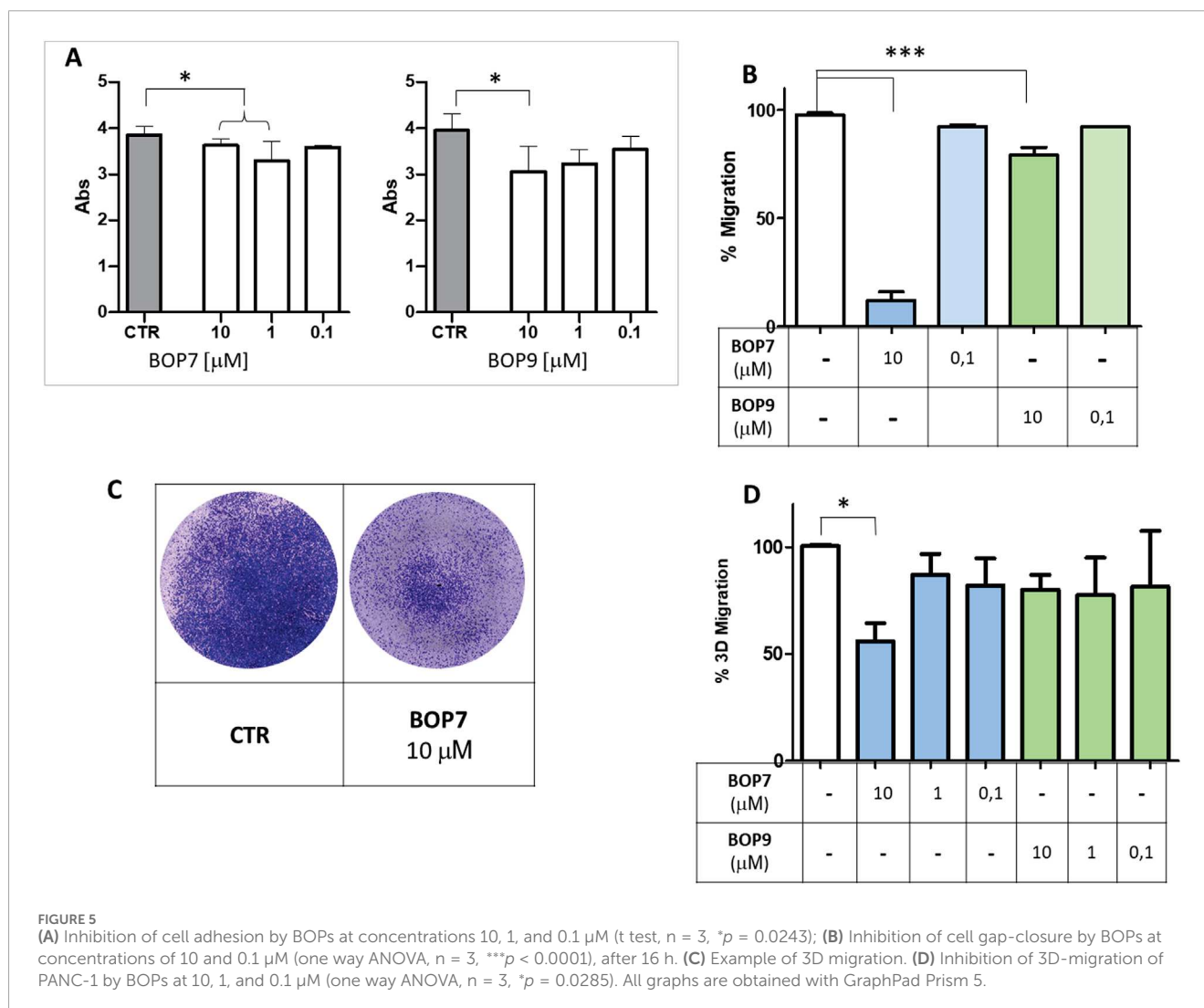
Immunogenic cell death inducers trigger release of HMGB1, which by binding to TLR4, promotes the processing and presentation of tumor antigens by inhibiting their premature lysosomal degradation (Apetoh et al., 2007a; Apetoh et al., 2007b). HMGB1 release was assessed by ELISA using the supernatants of PANC-1 cells treated for 24 h with the BOPs and chemotherapeutics at different concentrations (from 300 to 2 μ M). BOP7 and BOP9 induced greater release of HMGB1 than irinotecan at concentrations of 300 and 50 μ M, but less than daunorubicin, which proved to be the most effective inducer even at the lowest concentrations (Figure 6A).

IFN- β secretion

Immunogenic cell death inducers can stimulate the production of IFN- β type-1 interferon, which acts on its receptor (IFNAR1) and stimulates transcription of specific target genes activating a signal transduction cascade that in turn stimulates T cell recruitment (Sistigu et al., 2014; Ahmed and Tait, 2020). IFN- β secretion was assessed by ELISA using the supernatants of PANC-1 cells treated for 24 h with the different BOPs (Figure 5B). BOP7 and BOP9 at concentrations of 300 and 50 μ M significantly stimulated IFN- β secretion compared to untreated cells. In contrast, daunorubicin and irinotecan did not result in a statistically significant release of IFN- β (Figure 6B).

ATP release

The release of ATP is another hallmark of immunogenic cell death (Krysko et al., 2013). ATP release by PANC-1 cells after treatment with BOPs and chemotherapeutics at different concentrations (from 50 to 2 μ M), was measured using a bioluminescence test with luciferase. At a concentration of 50 μ M, daunorubicin was shown to be the most effective agent at inducing



ATP release (Figure 6C). However, the peak of ATP release was reached at 3 h, and after 6 h, release returned to baseline. In contrast, at the same concentration, BOP7 and BOP9 stimulated ATP release for longer. After 24 h, BOP7 and BOP9 at 50 and 20 μM released about twice as much ATP as daunorubicin and irinotecan (Figure 6D).

Mouse model of pancreatic cancer metastases

Considering the tumor-specific anticancer activity of the BOPs, their inhibitory activity in invasiveness/metastatic models *in vitro* and their resistance to circulating proteases, we studied their antitumor effect in a mouse model of metastases.

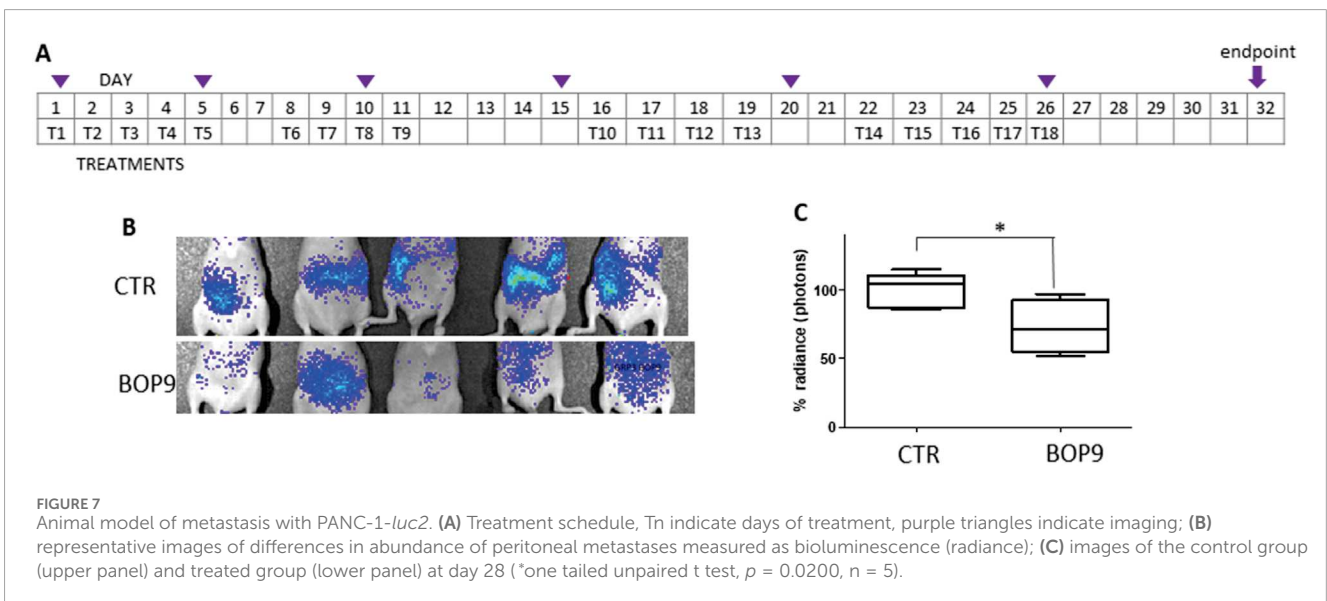
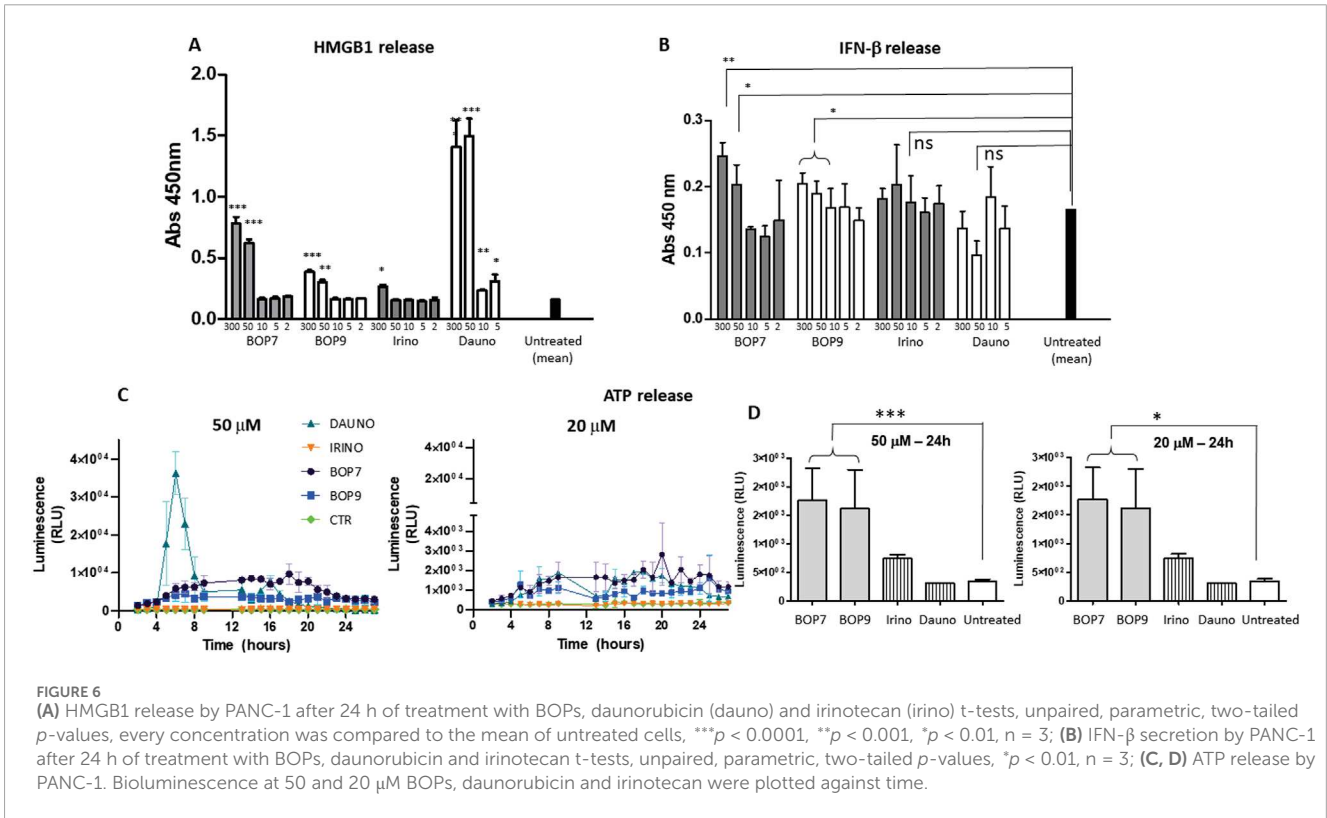
BALB-c nu/nu mice were injected in the caudal vein with $0.5\text{--}1 \times 10^6$ PANC1-*luc2* cells (Yuan et al., 2017). PANC1-*luc2* were obtained by transfection of PANC-1 with a plasmid DNA (PGL45LUC2CMVNEO) and proved to have the same susceptibility to BOPs as wild type PANC-1. BOP9 was initially selected for the

in vivo test because of its slightly lower cytotoxicity against non-cancer cells, compared to BOP7 ($\text{IC}_{50} 1.6 \times 10^{-2}$ M versus 5.0×10^{-3} M, against CHO-K1). Treatments were administered every day for the first 5 days, starting 4 h after transplant, followed by 2 days of interval, then three treatment cycles, with 2 day intervals were repeated for a total of 18 treatments over 32 days (Figure 7A). Tumor growth was monitored using an imaging system (IVIS, PerkinElmer) to capture bioluminescence images of the two groups of mice every 5–6 days (Figure 7B). The images were acquired on anesthetized mice, which were injected with luciferin 15 min prior to imaging. BOP9 reduced tumor metastasis growth by 20% with respect to untreated animals (Figure 7C).

Besides obtaining a reduction in tumor growth, BOPs proved to distribute systemically after intraperitoneal administration and to reach the site of the tumor or metastases.

Discussion

Tumors with an immunosuppressor microenvironment have poor prognosis. Pancreatic ductal adenocarcinoma is characterized



by a prevalence of immunosuppressive infiltrating cells, giving rise to one of the highest mortality rates among all cancer types: the 10-year overall survival rate is approximately 1% (Siegel et al., 2022). Strategies to neutralize the immunosuppressive stroma with high specificity are essential to improve the therapeutic statistics.

Immunogenic cell death (ICD) emerges as a promising solution and several clinical trials have reported a better overall response rate than to chemotherapy alone (Sprooten et al., 2023; Zhang et al., 2024; Islam et al., 2023; Galassi et al., 2024). Most

studies investigate the ICD-inducing effect of co-treatment with multiple common chemotherapeutics, such as anthracyclines, cyclophosphamide, oxaliplatin, paclitaxel, 5-fluorouracil and immune-check-point inhibitors (Jiang et al., 2021) or passive tumor-targeting immunotherapies, such as trastuzumab (anti-human epidermal growth factor receptor 2).

Peptides hold significant promise in this capacity and are poised to be extensively used in this context in the coming years, owing to their ease of preparation and availability.

Anticancer peptides have already been demonstrated to induce ICD (Ghaly et al., 2023; Pasquereau-Kotula et al., 2018).

Two peptides, BOP7 and BOP9, showed resistance to proteolysis, unlike their linear analogues. The promising cancer selectivity of the two BOP peptides is attributed to their repeated cationic sequences, which enable multivalent binding to HSPGs bearing multiple anionic sulfation patterns. Cancer cells typically show increased surface negativity due to increased presence of anionic components, such as the sulfate groups and carboxylic moieties of the glycosaminoglycan portion of HSPGs and sialic acid (Liu et al., 2023). HSPGs are a family of around twenty members, universally expressed in all eukaryotic cells. Many alterations in their expression are reported across different cancer types (Furini and Falciani, 2021; Proteinatlas, 2024). These alterations primarily affect the structure of the glycosaminoglycan chains and the expression levels of the proteoglycans. Both PANC-1 and Mia PaCa-2 cell lines express HSPGs (Furini and Falciani, 2021; Proteinatlas, 2024; Depau et al., 2020). The selectivity of the peptides towards cancer cells, observed when comparing PANC-1 or Mia PaCa-2 to the non-cancerous RAW264.7 and CHO cells, is most likely related to an increased expression of HSPGs in the tumor cells, modifications in the GAG chains, or modified arrangement of sulfations on the GAG chains in the pancreatic cancer cell lines (Kleeff et al., 1998; Uhlen et al., 2017).

This interaction of BOPs with HSPGs not only fosters an anti-metastatic effect *in vitro*, as shown by reduced adhesion and migration of PANC-1 cancer cells, but also demonstrates promising specific tumor cytotoxicity with low hemolytic activity. Remarkably, the cytotoxicity induced by BOPs triggers release of damage-associated molecular patterns (DAMPs), particularly HMGB1, IFN- β and ATP, by dying cells, and they persist for longer than conventional chemotherapeutic agents such as irinotecan and daunorubicin. The fact that they have a longer-lasting effect on DAMP-release makes BOPs excellent candidates for combined therapies that leverage immunogenic cell death. The *in vivo* assay in nude mice showed an encouraging ability of BOP9 to inhibit tumor grafting and metastasis growth in a pancreatic cancer model. In addition, BOP9 demonstrated systemic distribution after intraperitoneal administration and thus the ability to effectively reach tumor or metastatic sites, which is a crucial feature for further development.

In light of these promising preliminary results, further studies are needed to precisely define the potential activated pathways of these branched peptides and their mechanism for triggering the release of DAMPs to induce ICD. Additionally, investigating the efficacy of a combined treatment involving BOPs and other clinical standard chemotherapeutics, particularly immune checkpoint inhibitors (Schizas et al., 2020; Muller et al., 2022), will pave the way for developing new treatment options for non-responding, immunologically silent types of cancers.

Data availability statement

The raw data supporting the conclusions of this article will be made available by the authors, without undue reservation.

Ethics statement

Ethical approval was not required for the studies on humans in accordance with the local legislation and institutional requirements because only commercially available established cell lines were used. The animal study was approved by Animal Welfare Body (AWB) of Fondazione Toscana Life Sciences (FTLS). The study was conducted in accordance with the local legislation and institutional requirements.

Author contributions

AR: Writing–review and editing, Methodology, Investigation. ET: Writing–review and editing, Methodology, Investigation. GM: Writing–original draft, Methodology. JB: Writing–review and editing, Supervision. TH: Writing–review and editing, Validation, Data curation. AP: Writing–review and editing, Formal Analysis. LB: Writing–review and editing, Resources. CF: Writing–original draft, Supervision, Funding acquisition, Conceptualization.

Funding

The author(s) declare that financial support was received for the research, authorship, and/or publication of this article. This work was funded by Regione Toscana - Progetto Bando Ricerca Salute 2018 PANCREAS ED (CUP D73J20000040002).

Acknowledgments

The authors thank Silvia Scali and Stefano Bindi for their contribution. Figures contain elements from Biorender (<https://biorender.com>), allowed access on the 15/03/2024.

Conflict of interest

The authors declare that the research was conducted in the absence of any commercial or financial relationships that could be construed as a potential conflict of interest.

Publisher's note

All claims expressed in this article are solely those of the authors and do not necessarily represent those of their affiliated organizations, or those of the publisher, the editors and the reviewers. Any product that may be evaluated in this article, or claim that may be made by its manufacturer, is not guaranteed or endorsed by the publisher.

Supplementary material

The Supplementary Material for this article can be found online at: <https://www.frontiersin.org/articles/10.3389/fmolb.2024.1429163/full#supplementary-material>

References

- Ahmed, A., and Tait, S. W. G. (2020). Targeting immunogenic cell death in cancer. *Mol. Oncol.* 14 (12), 2994–3006. doi:10.1002/1878-0261.12851
- Alexandrov, L. B., Nik-Zainal, S., Wedge, D. C., Aparicio, S. A., Behjati, S., Biankin, A. V., et al. (2013). Signatures of mutational processes in human cancer. *Nature* 500 (7463), 415–421. doi:10.1038/nature12477
- Apetoh, L., Ghiringhelli, F., Tesniere, A., Criollo, A., Ortiz, C., Lidereau, R., et al. (2007b). The interaction between HMGB1 and TLR4 dictates the outcome of anticancer chemotherapy and radiotherapy. *Immunol. Rev.* 220, 47–59. doi:10.1111/j.1600-065X.2007.00573.x
- Apetoh, L., Ghiringhelli, F., Tesniere, A., Obeid, M., Ortiz, C., Criollo, A., et al. (2007a). Toll-like receptor 4-dependent contribution of the immune system to anticancer chemotherapy and radiotherapy. *Nat. Med.* 13 (9), 1050–1059. doi:10.1038/nm1622
- Bracci, L., Falciani, C., Lelli, B., Lozzi, L., Runci, Y., Pini, A., et al. (2003). Synthetic peptides in the form of dendrimers become resistant to protease activity. *J. Biol. Chem.* 278 (47), 46590–46595. doi:10.1074/jbc.M308615200
- Brunetti, J., Falciani, C., Lelli, B., Minervini, A., Ravenni, N., Depau, L., et al. (2015). Neurotensin branched peptide as a tumor-targeting agent for human bladder cancer. *Biomed. Res. Int.* 2015, 173507. doi:10.1155/2015/173507
- Chen, C. J., Tsai, K. C., Kuo, P. H., Chang, P. L., Wang, W. C., Chuang, Y. J., et al. (2015). A heparan sulfate-binding cell penetrating peptide for tumor targeting and migration inhibition. *Biomed. Res. Int.* 2015, 237969. doi:10.1155/2015/237969
- Depau, L., Brunetti, J., Falciani, C., Mandarini, E., Riolo, G., Zanchi, M., et al. (2020). Heparan sulfate proteoglycans can promote opposite effects on adhesion and directional migration of different cancer cells. *J. Med. Chem.* 63 (24), 15997–16011. doi:10.1021/acs.jmedchem.0c01848
- Di Federico, A., Mosca, M., Pagani, R., Carloni, R., Frega, G., De Giglio, A., et al. (2022). Immunotherapy in pancreatic cancer: why do we keep failing? A focus on tumor immune microenvironment, predictive biomarkers and treatment outcomes. *Cancers (Basel)* 14 (10), 2429. doi:10.3390/cancers14102429
- Esko, J. D., Rostand, K. S., and Weinke, J. L. (1988). Tumor formation dependent on proteoglycan biosynthesis. *Science* 241 (4869), 1092–1096. doi:10.1126/science.3137658
- Falciani, C., Brunetti, J., Lelli, B., Ravenni, N., Lozzi, L., Depau, L., et al. (2013). Cancer selectivity of tetra-branched neurotensin peptides is generated by simultaneous binding to sulfated glycosaminoglycans and protein receptors. *J. Med. Chem.* 56 (12), 5009–5018. doi:10.1021/jm400329p
- Falciani, C., Lozzi, L., Pini, A., Corti, F., Fabbrini, M., Bernini, A., et al. (2007). Molecular basis of branched peptides resistance to enzyme proteolysis. *Chem. Biol. Drug Des.* 69 (3), 216–221. doi:10.1111/j.1747-0285.2007.00487.x
- Feliu, L., Oliveras, G., Cirac, A. D., Besalú, E., Rosés, C., Colomer, R., et al. (2010). Antimicrobial cyclic decapeptides with anticancer activity. *Peptides* 31 (11), 2017–2026. doi:10.1016/j.peptides.2010.07.027
- Furini, S., and Falciani, C. (2021). Expression and role of heparan sulfated proteoglycans in pancreatic cancer. *Front. Oncol.* 11, 695858. doi:10.3389/fonc.2021.695858
- Galassi, C., Klapp, V., Yamazaki, T., and Galluzzi, L. (2024). Molecular determinants of immunogenic cell death elicited by radiation therapy. *Immunol. Rev.* 321 (1), 20–32. doi:10.1111/imr.13271
- Galluzzi, L., Buqué, A., Kepp, O., Zitvogel, L., and Kroemer, G. (2017). Immunogenic cell death in cancer and infectious disease. *Nat. Rev. Immunol.* 17 (2), 97–111. doi:10.1038/nri.2016.107
- Galluzzi, L., Vitale, I., Warren, S., Adjemian, S., Agostinis, P., Martinez, A. B., et al. (2020). Consensus guidelines for the definition, detection and interpretation of immunogenic cell death. *J. Immunother. Cancer* 8 (1), e000337. doi:10.1136/jitc-2019-000337
- Ghaly, G., Tallima, H., Dabbish, E., Badr ElDin, N., Abd El-Rahman, M. K., Ibrahim, M. A. A., et al. (2023). Anti-cancer peptides: status and future prospects. *Molecules* 28 (3), 1148. doi:10.3390/molecules28031148
- Gomes-da-Silva, L. C., Zhao, L., Bezu, L., Zhou, H., Sauvat, A., Liu, P., et al. (2018). Photodynamic therapy with redaporfin targets the endoplasmic reticulum and Golgi apparatus. *EMBO J.* 37 (13), e98354. doi:10.15252/embj.201798354
- Herting, C. J., Karpovsky, I., and Lesinski, G. B. (2021). The tumor microenvironment in pancreatic ductal adenocarcinoma: current perspectives and future directions. *Cancer Metastasis Rev.* 40 (3), 675–689. doi:10.1007/s10555-021-09988-w
- Hou, W., Yang, B., and Zhu, H. (2022). Nanoparticle-Based therapeutic strategies for enhanced pancreatic ductal adenocarcinoma immunotherapy. *Pharmaceutics* 14 (10), 2033. doi:10.3390/pharmaceutics14102033
- Islam, M. R., Patel, J., Back, P. I., Shmeeda, H., Kallem, R. R., Shudde, C., et al. (2023). Pegylated liposomal alendronate biodistribution, immune modulation, and tumor growth inhibition in a murine melanoma model. *Biomolecules* 13 (9), 1309. doi:10.3390/biom13091309
- Jiang, Y.-Z., Liu, Y., Xiao, Y., Hu, X., Jiang, L., Zuo, W.-J., et al. (2021). Molecular subtyping and genomic profiling expand precision medicine in refractory metastatic triple-negative breast cancer: the FUTURE trial. *Cell Res.* 31, 178–186. doi:10.1038/s41422-020-0375-9
- Kleeff, J., Ishiwata, T., Kumbasar, A., Friess, H., Büchler, M. W., Lander, A. D., et al. (1998). The cell-surface heparan sulfate proteoglycan glypican-1 regulates growth factor action in pancreatic carcinoma cells and is overexpressed in human pancreatic cancer. *J. Clin. Invest.* 102 (9), 1662–1673. doi:10.1172/JCI4105
- Kroemer, G., Galassi, C., Zitvogel, L., and Galluzzi, L. (2022). Immunogenic cell stress and death. *Nat. Immunol.* 23 (4), 487–500. doi:10.1038/s41590-022-01132-2
- Krysko, O., Løve Aaes, T., Bachert, C., Vandenabeele, P., and Krysko, D. V. (2013). Many faces of DAMPs in cancer therapy. *Cell Death Dis.* 4 (5), e631. doi:10.1038/cddis.2013.156
- Li, X., Zhong, H., Zheng, S., Mu, J., Yu, N., and Guo, S. (2024). Tumor-penetrating iRGD facilitates penetration of poly(floxuridine-ketal)-based nanomedicine for enhanced pancreatic cancer therapy. *J. Control Release* 369, 444–457. doi:10.1016/j.jconrel.2024.04.004
- Liu, H., Shen, W., Liu, W., Yang, Z., Yin, D., and Xiao, C. (2023). From oncolytic peptides to oncolytic polymers: a new paradigm for oncotherapy. *Bioact. Mater* 31, 206–230. doi:10.1016/j.bioactmat.2023.08.007
- Monroc, S., Badosa, E., Besalú, E., Planas, M., Bardaji, E., Montesinos, E., et al. (2006). Improvement of cyclic decapeptides against plant pathogenic bacteria using a combinatorial chemistry approach. *Peptides* 27 (11), 2575–2584. doi:10.1016/j.peptides.2006.05.001
- Muller, M., Haghnejad, V., Schaefer, M., Gauchotte, G., Caron, B., Peyrin-Biroulet, L., et al. (2022). The immune landscape of human pancreatic ductal carcinoma: key players, clinical implications, and challenges. *Cancers (Basel)* 14 (4), 995. doi:10.3390/cancers14040995
- Nielsen, M., Monberg, T., Sundvold, V., Albieri, B., Hovgaard, D., Petersen, M. M., et al. (2023). LTX-315 and adoptive cell therapy using tumor-infiltrating lymphocytes generate tumor specific T cells in patients with metastatic soft tissue sarcoma. *Oncoimmunology* 13 (1), 2290900. doi:10.1080/2162402X.2023.2290900
- Pasquereau-Kotula, E., Habault, J., Kroemer, G., Poyet, J.-L., and Ma, W.-L. (2018). The anticancer peptide RT53 induces immunogenic cell death. *PLoS One* 13, e0201220. doi:10.1371/journal.pone.0201220
- Paul, S., Verma, S., and Chen, Y. C. (2024). Peptide dendrimer-based antibacterial agents: synthesis and applications. *ACS Infect. Dis.* 10, 1034–1055. doi:10.1021/acsinfecdis.3c00624
- Proteinatlas (2024). Available at: <https://www.proteinatlas.org/search/proteoglycan> (Accessed July 17, 2024).
- Schizas, D., Charalampakis, N., Kole, C., Economopoulou, P., Koustas, E., Gkotsis, E., et al. (2020). Immunotherapy for pancreatic cancer: a 2020 update. *Cancer Treat. Rev.* 86, 102016. doi:10.1016/j.ctrv.2020.102016
- Shekarian, T., Sivad, E., Jallas, A. C., Depil, S., Kielbassa, J., Janoueix-Lerosey, I., et al. (2019). Repurposing rotavirus vaccines for intratumoral immunotherapy can overcome resistance to immune checkpoint blockade. *Sci. Transl. Med.* 11 (515), eaat5025. doi:10.1126/scitranslmed.aat5025
- Siegel, R. L., Miller, K. D., Fuchs, H. E., and Jemal, A. (2022). Cancer statistics, 2022. *CA Cancer J. Clin.* 72 (1), 7–33. doi:10.3322/caac.21708
- Sistigu, A., Yamazaki, T., Vacchelli, E., Chaba, K., Enot, D. P., Adam, J., et al. (2014). Cancer cell-autonomous contribution of type I interferon signaling to the efficacy of chemotherapy. *Nat. Med.* 20 (11), 1301–1309. doi:10.1038/nm.3708
- Sprooten, J., Laureano, R. S., Vanmeerbeek, I., Govaerts, J., Naulaerts, S., Borrás, D. M., et al. (2023). Trial watch: chemotherapy-induced immunogenic cell death in oncology. *Oncoimmunology* 12 (1), 2219591. doi:10.1080/2162402X.2023.2219591
- Tornesello, A. L., Borrelli, A., Buonaguro, L., Buonaguro, F. M., and Tornesello, M. L. (2020). Antimicrobial peptides as anticancer agents: functional properties and biological activities. *Molecules* 25 (12), 2850. doi:10.3390/molecules25122850
- Uhlen, M., Zhang, C., Lee, S., Sjöstedt, E., Fagerberg, L., Bidkhori, G., et al. (2017). A pathology atlas of the human cancer transcriptome. *Science* 357 (6352), eaan2507. doi:10.1126/science.aan2507
- Yamazaki, T., Buqué, A., Ames, T. D., and Galluzzi, L. (2020). PT-112 induces immunogenic cell death and synergizes with immune checkpoint blockers in

mouse tumor models. *Oncoimmunology* 9 (1), 1721810. doi:10.1080/2162402X.2020.1721810

Yang, H., and Wang, L. (2023). Heparan sulfate proteoglycans in cancer: pathogenesis and therapeutic potential. *Adv. Cancer Res.* 157, 251–291. doi:10.1016/bs.acr.2022.08.001

Yin, C., Alqahtani, A., and Noel, M. S. (2022). The next frontier in pancreatic cancer: targeting the tumor immune milieu and molecular pathways. *Cancers (Basel)* 14 (11), 2619. doi:10.3390/cancers14112619

Yuan, P., He, X. H., Rong, Y. F., Cao, J., Li, Y., Hu, Y. P., et al. (2017). KRAS/NF- κ B/YY1/miR-489 signaling Axis controls pancreatic cancer

metastasis. *Cancer Res.* 77 (1), 100–111. doi:10.1158/0008-5472.CAN-16-1898

Zhang, B., Li, N., Gao, J., Zhao, Y., Jiang, J., Xie, S., et al. (2024). Targeting of focal adhesion kinase enhances the immunogenic cell death of PEGylated liposome doxorubicin to optimize therapeutic responses of immune checkpoint blockade. *J. Exp. Clin. Cancer Res.* 43 (1), 51. doi:10.1186/s13046-024-02974-4

Zhou, J., Wang, G., Chen, Y., Wang, H., Hua, Y., and Cai, Z. (2019). Immunogenic cell death in cancer therapy: present and emerging inducers. *J. Cell Mol. Med.* 23 (8), 4854–4865. doi:10.1111/jcmm.14356